

AGU Advances



RESEARCH ARTICLE

10.1029/2023AV000911

Peer Review The peer review history for this article is available as a PDF in the Supporting Information.

Key Points:

- Chemical feedbacks from stratospheric aerosol injection, a form of solar geoengineering, increase tropospheric oxidative capacity
- Atmospheric composition changes due to geoengineering substantially influence the resulting seasonal and spatial patterns of radiative forcing
- The level of stratospheric ozone depletion seen from geoengineering leads to a decline in global mortality, driven by air pollution changes

Supporting Information:

Supporting Information may be found in the online version of this article.

Correspondence to:

J. M. Moch,
research@jmoch.net

Citation:

Moch, J. M., Mickley, L. J., Eastham, S. D., Lundgren, E. W., Shah, V., Buonocore, J. J., et al. (2023). Overlooked long-term atmospheric chemical feedbacks alter the impact of solar geoengineering: Implications for tropospheric oxidative capacity. *AGU Advances*, 4, e2023AV000911. <https://doi.org/10.1029/2023AV000911>

Received 2 MAR 2023

Accepted 3 AUG 2023

Author Contributions:

Conceptualization: Jonathan M. Moch, Loretta J. Mickley, Sebastian D. Eastham, Jonathan J. Buonocore








Formal analysis: Jonathan M. Moch, Loretta J. Mickley, Viral Shah, Mehliyar Sadiq

Funding acquisition: Jonathan M. Moch, Loretta J. Mickley

© 2023. The Authors.

This is an open access article under the terms of the [Creative Commons Attribution License](https://creativecommons.org/licenses/by/4.0/), which permits use, distribution and reproduction in any medium, provided the original work is properly cited.

Overlooked Long-Term Atmospheric Chemical Feedbacks Alter the Impact of Solar Geoengineering: Implications for Tropospheric Oxidative Capacity

Jonathan M. Moch^{1,2,3} , Loretta J. Mickley¹ , Sebastian D. Eastham⁴ , Elizabeth W. Lundgren¹, Viral Shah^{1,5,6}, Jonathan J. Buonocore^{2,7} , Jacky Y. S. Pang^{8,9} , Mehliyar Sadiq⁸ , and Amos P. K. Tai^{8,10} 

¹John A. Paulson School of Engineering and Applied Sciences, Harvard University, Cambridge, MA, USA, ²Center for Climate, Health, and the Global Environment, T.H. Chan School of Public Health, Harvard University, Boston, MA, USA, ³Now at AAAS Science and Technology Policy Fellowship Program at U.S. Department of State, Washington, DC, USA, ⁴Laboratory for Aviation and the Environment, Department of Aeronautics and Astronautics, Massachusetts Institute of Technology, Cambridge, MA, USA, ⁵Now at Global Modeling and Assimilation Office, NASA Goddard Space Flight Center, Greenbelt, MD, USA, ⁶Now at Science System and Applications, Inc, Lanham, MD, USA, ⁷Now at Boston University School of Public Health, Boston, MA, USA, ⁸Institute of Environment, Energy and Sustainability, The Chinese University of Hong Kong, Sha Tin, Hong Kong, ⁹Now at Institute of Energy and Climate Research, IEK-8: Troposphere, Forschungszentrum Jülich GmbH, Jülich, Germany, ¹⁰Earth System Science Programme, Faculty of Science, State Key Laboratory of Agrobiotechnology, The Chinese University of Hong Kong, Sha Tin, Hong Kong

Abstract Studies of the impacts of solar geoengineering have mostly ignored tropospheric chemistry. By decreasing the sunlight reaching Earth's surface, geoengineering may help mitigate anthropogenic climate change, but changing sunlight also alters the rates of chemical reactions throughout the troposphere. Using the GEOS-Chem atmospheric chemistry model, we show that stratospheric aerosol injection (SAI) with sulfate, a frequently studied solar geoengineering method, can perturb tropospheric composition over a span of 10 years, increasing tropospheric oxidative capacity by 9% and reducing methane lifetime. SAI decreases the overall flux of shortwave radiation into the troposphere, but increases flux at certain UV wavelengths due to stratospheric ozone depletion. These radiative changes, in turn, perturb tropospheric photochemistry, driving chemical feedbacks that can substantially influence the seasonal and spatial patterns of radiative forcing beyond what is caused by enhanced stratospheric aerosol concentrations alone. For example, chemical feedbacks decrease the radiative effectiveness of geoengineering in northern high latitude summer by 20%. Atmospheric chemical feedbacks also imply the potential for net global public health benefits associated with stratospheric ozone depletion, as the decreases in mortality resulting from SAI-induced improvements in air quality outweigh the increases in mortality due to increased UV radiation exposure. Such chemical feedbacks also lead to improved plant growth. Our results show the importance of including fuller representations of atmospheric chemistry in studies of solar geoengineering and underscore the risk of surprises from this technology that could carry unexpected consequences for Earth's climate, the biosphere, and human health.

Plain Language Summary Solar geoengineering is a proposed set of technologies to help lessen the impacts of climate change by reducing the amount of sunlight received by the Earth. Stratospheric aerosol injection is a method of solar geoengineering that reduces sunlight by increasing the amount of aerosol particles in the stratosphere, a process which can also cause stratospheric ozone depletion. Nearly all studies of stratospheric aerosol injection have focused exclusively on the direct impacts of increased stratospheric aerosol on climate. However, changes in sunlight also alter the rates of chemical reactions throughout the atmosphere, changing the concentrations of greenhouse gases that affect climate like methane and tropospheric ozone. Our results show that these changes in greenhouse gases due to geoengineering chemical feedbacks can substantially alter the climate effect of geoengineering, especially on regional and seasonal scales. Our results also show that geoengineering-induced stratospheric ozone depletion can lead to net global health benefits, as the impacts on mortality from overall improvements in surface air quality due to chemical feedbacks outweigh those from increases in UV exposure. These same chemical feedbacks can also improve crop yields and overall plant growth. Our results underscore the risk of surprises that could arise from solar geoengineering.

Investigation: Jonathan M. Moch, Sebastian D. Eastham, Viral Shah, Jonathan J. Buonocore, Jacky Y. S. Pang, Mehliyar Sadiq, Amos P. K. Tai
Methodology: Jonathan M. Moch, Loretta J. Mickley, Sebastian D. Eastham, Elizabeth W. Lundgren, Jonathan J. Buonocore, Jacky Y. S. Pang, Mehliyar Sadiq, Amos P. K. Tai
Resources: Loretta J. Mickley
Software: Jonathan M. Moch, Sebastian D. Eastham, Elizabeth W. Lundgren, Viral Shah, Jacky Y. S. Pang, Mehliyar Sadiq, Amos P. K. Tai
Supervision: Jonathan M. Moch, Loretta J. Mickley, Sebastian D. Eastham, Viral Shah, Amos P. K. Tai
Validation: Jonathan J. Buonocore
Visualization: Jonathan M. Moch
Writing – original draft: Jonathan M. Moch, Loretta J. Mickley
Writing – review & editing: Jonathan M. Moch, Loretta J. Mickley, Sebastian D. Eastham, Elizabeth W. Lundgren, Viral Shah, Jonathan J. Buonocore, Jacky Y. S. Pang, Mehliyar Sadiq, Amos P. K. Tai

1. Introduction

Stratospheric aerosol injection (SAI) is a proposed method of solar geoengineering. The goal of solar geoengineering is to mitigate anthropogenic climate change and therefore reduce the resulting harm, allowing time for humanity to decrease the atmospheric burden of greenhouse gases (Crutzen, 2006; Irvine & Keith, 2020; Irvine et al., 2016; Lee et al., 2021; National Academies of Science, Engineering and Medicine, 2021). SAI would accomplish this goal by increasing the concentration of aerosol particles in the stratosphere, with the majority of SAI studies considering the use of sulfate. This increase in aerosol abundance would reflect incoming solar radiation, thereby counteracting the radiative forcing by greenhouse gases and reducing surface temperatures (Irvine et al., 2016; Lee et al., 2021; National Academies of Science, Engineering and Medicine, 2021). Solar geoengineering methods are not substitutes for reducing greenhouse gas emissions and do not perfectly compensate for increases in greenhouse gas concentrations. Nevertheless, multiple modeling studies have suggested that SAI may be able to reduce global average surface temperatures and moderate the worst impacts of unabated climate change (Irvine et al., 2019; Keith & Irvine, 2016; Kravitz et al., 2017, 2021; Tilmes et al., 2013; Xu et al., 2020). Prior studies have found that SAI with sulfate aerosol can lead to various levels and patterns of stratospheric ozone depletion, including through enhancements in stratospheric heterogeneous chemistry (Pitari et al., 2014; Tilmes et al., 2009; Weisenstein et al., 2022). Alternative SAI methods, such as using calcite aerosol, have been proposed as a way to implement SAI without ozone depletion (Keith et al., 2016; Weisenstein et al., 2015). However, few studies have examined in detail the impact of SAI on tropospheric chemistry and composition. In particular, the consequences of SAI for the oxidative capacity of the troposphere remain a major uncertainty.

Sunlight is the key driver of the tropospheric photochemical system, responsible for both the generation and destruction of various oxidants which drive much of the chemical transformation of compounds in the atmosphere (Jacob, 2000). Changes in incoming sunlight due to geoengineering would thus likely influence tropospheric chemistry, changing the concentrations of aerosols and greenhouse gases. Due to the presence of long-lived and chemically important species such as methane (Szopa, et al., 2021), atmospheric composition may then continually change for years if geoengineering is sustained. This long response time suggests a shortcoming of using volcanic eruptions as analogs for solar geoengineering (Duan et al., 2019; Trenberth & Dai, 2007) since continuous sulfur injection forces the atmosphere to a new chemical equilibrium, while volcanoes are transitory events (McCormick et al., 1995).

Consideration of chemistry-climate feedbacks may be especially relevant to assessments of geoengineering compared to typical climate simulations. For computational expediency, most climate modeling to date has either not included interactive tropospheric chemistry or has used simple chemical schemes with limited dependence on changes in sunlight (Mills et al., 2017; Pitari et al., 2002; Schmidt et al., 2006). The majority of solar geoengineering simulations have also used such models (Irvine & Keith, 2020; Irvine et al., 2019; Kravitz et al., 2017, 2021; Pitari et al., 2014; Tilmes et al., 2009, 2013, 2018; Xu et al., 2020), meaning changes in chemistry affecting tropospheric aerosols and greenhouse gases are not captured. In standard climate modeling experiments involving greenhouse gases, these simple schemes can prove adequate. However, for solar geoengineering it is plausible that the radiative effect could be either significantly enhanced or limited by chemical responses. Changes in atmospheric composition could also modify the impact of geoengineering on air quality, human health, crop yields, or ecosystem health (Dagon & Schrag, 2019; Fan et al., 2021; National Academies of Sciences, Engineering and Medicine, 2021; Pitari et al., 2014; Proctor et al., 2018; Szopa et al., 2021; Tai & Val Martin, 2017; Tilmes et al., 2009; Tracy et al., 2022; Vioni et al., 2020; Vorha et al., 2021).

Despite their potential importance, chemical feedbacks remain little examined within the context of solar geoengineering. Of the numerous studies on SAI, we are aware of only three studies that have included a focus on tropospheric chemistry (Eastham, Weisenstein, et al., 2018; Vioni et al., 2017; Xia et al., 2017). Two of these models neglected key chemical processes important for simulating tropospheric chemistry and its response to geoengineering (Aquila et al., 2012; Pitari et al., 2002, 2014; Vioni et al., 2017; Xia et al., 2017), and all three ignored long-term feedbacks involving methane, a key greenhouse gas. The full suite of chemical feedbacks and driving mechanisms from geoengineering, especially those involving tropospheric processes, have thus yet to be comprehensively explored.

Here we identify the long-term chemical feedbacks from sulfate SAI that operate throughout both the stratosphere and troposphere, and we show how these feedbacks may alter the impacts of SAI. In particular, we investigate the

effects of these feedbacks on net radiative forcing, air quality, vegetation (including crop yields), acid rain, and the surface flux of ultraviolet (UV) radiation. We also examine the consequences of SAI on the oxidative capacity of the troposphere. This issue has importance as the oxidative capacity determines the lifetime of many tropospheric pollutants including methane (Alexander & Mickley, 2015). Finally, we evaluate the public health consequences of the change in human exposure to two key air pollutants—ozone and fine particulate matter (PM_{2.5})—and to UV radiation.

2. Materials and Methods

2.1. GEOS-Chem Model Set Up

For atmospheric chemistry simulations we use version 13.0.0 of the high-performance version of the GEOS-Chem chemical transport model (GCHP; <https://doi.org/10.5281/zenodo.4429193>) (Eastham, Long, et al., 2018; International GEOS-Chem User Community, 2021). GEOS-Chem includes fully coupled tropospheric and stratospheric HO_x-NO_x-VOC-ozone-halogen-aerosol chemistry for both gas and aqueous phases (Alexander et al., 2012; Eastham et al., 2014; Park et al., 2004; Shewen et al., 2016; Travis et al., 2016). Photolysis rates are calculated using the FAST-JX photolysis scheme (Bian & Prather, 2002; Eastham et al., 2014; Mao et al., 2010). We conduct two 10-year simulations using c48 horizontal resolution ($\sim 2^\circ$ latitude \times 2.5° longitude). To minimize meteorological variability and better isolate the photochemical response to SAI, each of the 10 simulation years is driven by 2016 meteorological fields from the GEOS-FP data assimilation product (Rienecker et al., 2008). All simulations rely on the same biogenic VOC emissions inventory and on a simple secondary organic aerosol (SOA) scheme which does not explicitly include cloud processing of SOA but nevertheless well reproduces the impact of aqueous phase SOA processing for present-day conditions (Guenther et al., 2012; Pai et al., 2020).

The standard version of GEOS-Chem uses a surface boundary condition for methane concentrations based on observations (Murray, 2016). In order to simulate the methane response to changes in oxidants and allow for tropospheric methane-OH feedbacks, here we generate a methane pseudo-emissions inventory, following an approach used for a different gas (Moch et al., 2018). We first simulate 5 years using the surface boundary condition, at which point the model has reached chemical equilibrium. For the next 5 years of simulation we archive the methane pseudo-flux, which is the flux needed to return surface methane concentrations to the boundary condition values. We then take the average flux for each month across these 5 years to create a monthly gridded climatology of methane pseudo emissions. We degrade the resolution of this inventory to 30° latitude bands. When used in lieu of the standard boundary condition, we find the pseudo-emissions reproduces reasonable (<5% error) surface methane concentrations in a non-perturbed simulation.

To implement stratospheric aerosol injection in GCHP, we use prescribed fields of stratospheric sulfate aerosol concentration and properties prepared for the G4 specified stratospheric aerosol experiment of the Geoengineering Modeling Intercomparison Project (GeoMIP) (Tilmes et al., 2015). The G4-SSA scenario is similar to the GeoMIP G4 scenario, which used a baseline scenario of RCP4.5 (Kravitz et al., 2011), but unlike G4, G4-SSA defines a fixed prescribed stratospheric aerosol distribution that is not tied to a specific baseline scenario and is also meant to be used in time slice experiments such as the one conducted here. The G4-SSA fields were generated based on a continuous tropical injection of 8 Tg SO₂ yr⁻¹ and were designed for use in climate and chemistry models for multi-model comparisons of the effect of stratospheric aerosol injection. This climatology consists of the monthly averages of these fields from the middle 10 years of the 54-year G4-SSA time series, where the stratospheric sulfur burden approaches an equilibrium of ~ 2 Tg S. For each chemical time step in GEOS-Chem, we overwrite the default values of stratospheric sulfate concentration, stratospheric liquid aerosol surface area density, and stratospheric liquid aerosol volume with the values from the monthly G4-SSA climatology. To examine the impact of stratospheric aerosol injection on atmospheric composition and second order impacts of SAI, we compare the simulation where stratospheric aerosol concentrations and properties are overwritten with a simulation with no changes to the standard model other than the treatment of methane emissions described previously. For each 10-year simulation we treat the first 5 years as spin up and analyze only years 6–10, when the model has reached chemical equilibrium.

2.2. Radiative Forcing Calculation

Radiative forcing is calculated online using the Rapid Radiative Transfer Model for GCMs (RRTMG; Iacono et al., 2008) coupled to GEOS-Chem (Heald et al., 2014). Unless otherwise indicated, radiative forcing refers

to the instantaneous change in forcing at the tropopause without considering stratospheric or other adjustment. RRTMG as implemented in GEOS-Chem calculates radiative forcing changes due to stratospheric and tropospheric aerosols, methane, ozone, nitrous oxide, carbon dioxide, oxygen, CFC11, CFC12, CCl4, and HCFC22. Perturbations to water vapor arising from chemical feedbacks are not considered in the radiative forcing calculations. Radiative forcing due to stratospheric aerosol injection (SAI) including and excluding chemical feedbacks is calculated as the difference between the net radiative fluxes between the geoengineering scenario and the control simulation (in which stratospheric aerosols are not modified). SAI radiative forcing for stratospheric aerosols only is calculated as the difference in stratospheric aerosol radiative forcing. SAI radiative forcing with chemical feedbacks considers the changes due to all radiatively active components. We also isolate the radiative effect of chemical feedbacks of SAI by subtracting the radiative forcing attributable to stratospheric aerosol only from the radiative forcing due to SAI including these feedbacks.

2.3. Public Health Calculations

Public health impacts of ozone, PM_{2.5}, and UV exposure are calculated as in Eastham, Weisenstein, et al. (2018), but with updates to the PM_{2.5} dose-response function (Vodonos et al., 2018). Impacts are calculated by conducting a Monte-Carlo simulation on dose response functions for fine particulate matter (PM_{2.5}), ozone, and ultraviolet (UV) radiation exposure. A triangular distribution is fit to the 95% confidence interval reported for the concentration response function parameters for each health outcome. Each Monte-Carlo simulation then includes 1000 draws for the key uncertain parameters in the dose response functions. We first calculate baseline mortality associated with population exposure in the control simulation by taking a country's mortality rate due to relevant diseases, in the appropriate age brackets, from World Health Organization data for 2016 and multiplying the rates by 2015 population data from the Gridded Population of the World v4.11 estimate (Center for International Earth Science Information Network, 2018). Change in mortality in the geoengineering scenario is calculated using the dose response functions to calculate the relative risk of mortality with and without the stratospheric aerosol enhancement, calculating the expected mortality in each scenario, and then taking the difference between the control and geoengineering simulations. Calculations of mortality from PM_{2.5} exposure use an all-cause mortality concentration response function (Vodonos et al., 2018), a meta-analysis of the epidemiological literature that provides a quantitative representation of the relationship between changes in annual average PM_{2.5} exposure and risk of mortality. This response function includes a modest saturation effect at high exposure levels and is applied to all ages. Ultraviolet exposure is calculated using a power-law relationship (Slaper et al., 1996). UV exposure data are weighted using SCUP-h (Spectrum Combined Utrecht/Philadelphia data, corrected for Human transmission), which weights the increase in exposure at different UV wavelengths according to the likely effect on human health. Ozone mortality is calculated using a log-linear concentration response function applied to population over the age of 30, calibrated with the ozone-season respiratory disease mortality data (Jerrett et al., 2009).

2.4. Gross Primary Productivity Calculations

To evaluate the impacts of geoengineering on global gross-primary production (GPP), simulations are conducted with the Terrestrial Ecosystem Model in R (TEMIR; Tai et al., 2021, 2023). The model computes the biogeophysical responses of terrestrial ecosystems to the changes in the terrestrial and atmospheric environment, including changes in ozone concentrations. TEMIR uses 24 plant function types (PFTs), with photosynthesis and stomatal conductance calculated for each PFT using the Farquhar-Ball-Berry model (Oleson et al., 2013).

Multiple ozone damage parameterization schemes are available in TEMIR. Here ozone damage on plants is parameterized with the damage dependent on the instantaneous stomatal uptake of ozone (F_{O_3}) (Sitch et al., 2007):

$$F_{O_3} = \frac{[O_3]}{R_a + R_b + 1.61 \times r_s}$$

where $[O_3]$ is the surface ozone concentration (nmol m^{-3}), R_a is the aerodynamic resistance (s m^{-1}), R_b is the boundary layer resistance (s m^{-1}), and r_s is the stomatal resistance (s m^{-1}). Accounting for ozone tolerance in plants with a critical threshold only above which ozone damage would accumulate (F_{crit} , $\text{nmol m}^{-2} \text{s}^{-1}$), the photosynthetic damage factor f is calculated as follows:

$$f = 1 - b \times \max[(F_{O_3} - F_{\text{crit}}), 0]$$

Table 1
 Plant-Specific Ozone Tolerance and Sensitivity Parameters Used in This Study^a

	Broadleaf trees ^b	Needleleaf trees ^c	C3 grasses ^d	C4 grasses ^e	Shrubs ^f
F_{crit} (nmol m ⁻² s ⁻¹)	1.6	1.6	5.0	5.0	1.6
$b_{\text{high sensitivity}}$ (nmol ⁻¹ m ² s)	0.15	0.075	1.40	0.735	0.10
$b_{\text{low sensitivity}}$ (nmol ⁻¹ m ² s)	0.04	0.02	0.25	0.13	0.03

^aParameters are from Sitch et al. (2007). ^b“Broadleaf Trees” refers to the eight broadleaf tree PFTs in the Community Land Model version 4.5 (CLM) (Oleson et al., 2013). ^c“Needleleaf Trees” refers to the three needleleaf trees PFTs in the CLM. ^d“C3 grasses” includes these PFTs: C₃ grass, C₃ arctic grass, C₃ unmanaged rainfed/irrigated crop, rainfed/irrigated temperate cereals, rainfed/irrigated winter cereals, and rainfed/irrigated soybean. ^e“C4 grasses” includes C₄ grass as well as rainfed/irrigated corn. ^f“Shrubs” refers to the three shrub PFTs in the CLM.

where b (nmol⁻¹ m² s) is the plant-specific parameter for ozone sensitivity (Table 1). The factor f is then multiplied by the net photosynthetic rate A_n to represent ozone damage and the effect on stomatal conductance g_s (i.e., r_s^{-1}).

TEMIR simulations are driven by hourly meteorological data at 2° latitude × 2.5° longitude resolution in the year 2016, using the Modern Era-Retrospective Analysis for Research and Applications version 2 (MERRA-2) reanalysis product (<https://gmao.gsfc.nasa.gov/reanalysis/MERRA-2/>). Atmospheric CO₂ concentration is set to 400 ppm. Simulations are performed with hourly mean ozone concentrations averaged over 5 years. To isolate the effect of changing ozone on GPP, the incoming solar radiation received by terrestrial ecosystems is kept constant in the TEMIR simulations. We calculate four scenarios of ozone damage to vegetation: with and without SAI and with high and low plant-ozone sensitivities (Table 1).

2.5. Crop Yield Calculations

The impact of ozone changes on global crop production are estimated using the concentration-response function for AOT40, which is a cumulative ozone exposure metric calculated from hourly mean concentrations of surface ozone (Tai et al., 2014, 2021).

The AOT40 cumulative exposure metric (in unit of ppm-h) is:

$$\text{AOT40} = \sum_{i=1}^n ([\text{O}_3]_i - 0.04)$$

where $[\text{O}_3]$ is the hourly mean surface ozone concentration (ppm) during the 12 hr of local daylight (8:00–19:59) and n is the number of hours in the 3-month growing season prior to the start of harvest. Relationships between ozone exposure and crop yield are listed in Table 2.

Base crop yields are based on data for 2016 (Iizumi & Sakai, 2020). Crop calendar data, indicating when during the year crops are harvested, are from Sacks et al. (2010) and from harvest area originally compiled by Tai et al. (2014). Changes in crop yield due to SAI are determined as the difference in crop yield loss due to ozone exposure between the SAI scenario and the control scenario. As with GPP, the incoming solar radiation received by crops is kept constant to isolate the effect of changing ozone concentrations. These changes are converted from tons to equivalent food energy using the values in Table 2.

Table 2
 AOT40 Ozone Exposure-Yield Relationships and Crop Caloric Values

Crop	AOT40 relationship ^a	Equivalent food energy (10 ⁶ kcal ton ⁻¹) ^b
Wheat	$\text{RY} = 1 - 0.0163 \times \text{AOT40}$	3.34
Rice	$\text{RY} = 1 - 0.00415 \times \text{AOT40}$	3.63
Maize	$\text{RY} = 1 - 0.00356 \times \text{AOT40}$	3.65
Soybean	$\text{RY} = 1 - 0.0113 \times \text{AOT40}$	4.46

^aRY is the yield ratio, where $\text{RY} = Y/Y_0$, Y is the yield, and Y_0 is the maximum potential yield with zero ozone exposure. AOT40 relationships are from Van Dingenen et al. (2009). ^bEquivalent food energy values from the U.S. Department of Agriculture National Nutrient Database for Standard Reference (<http://ndb.nal.usda.gov>).

2.6. Acid Precipitation Calculations

Changes in acid precipitation are calculated using monthly mean wet deposition fluxes and precipitation volume (Shah et al., 2020). The calculation uses archived precipitation volume and wet deposition fluxes for sulfate, nitrate, chloride, carboxylic acids, ammonium, and nonvolatile cations in dust and sea salt aerosols. The CO₂ mixing ratio is set to 390 ppm. Acid flux to ecosystems, both land and oceanic, is calculated assuming nitrogen-limited and

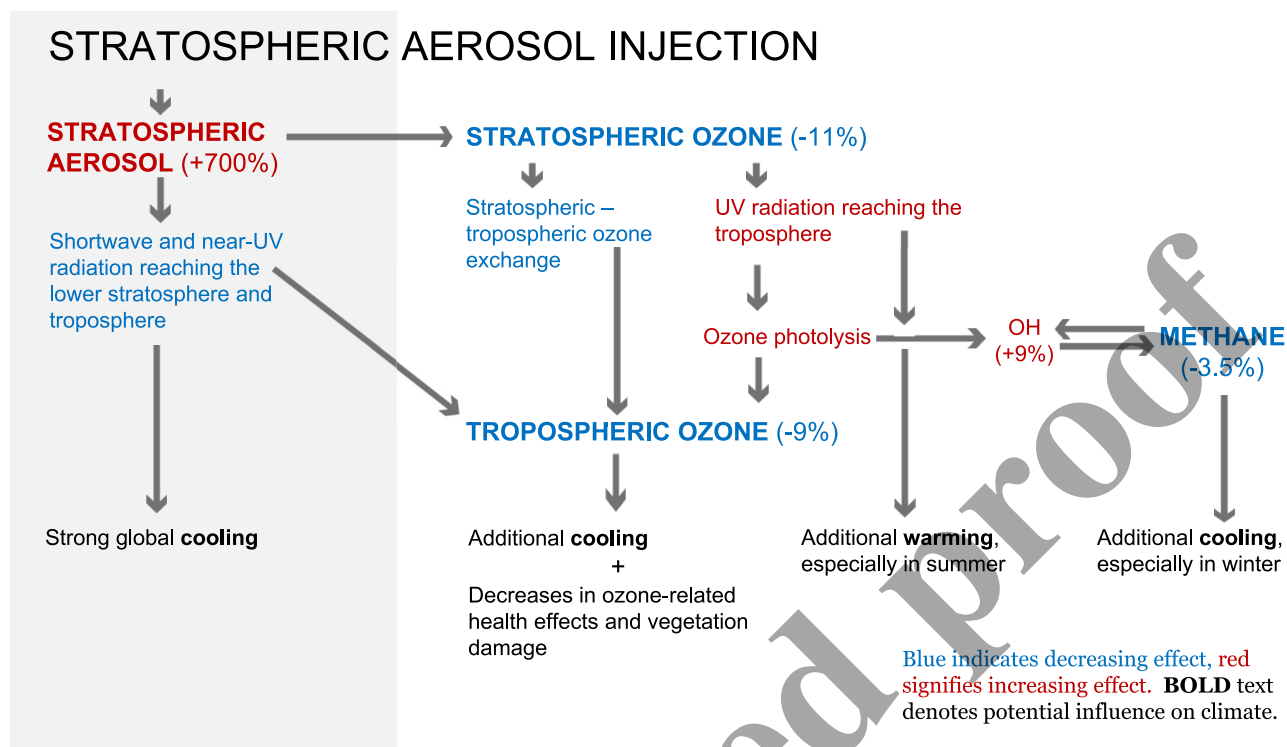


Figure 1. Diagram of major atmospheric chemistry changes and mechanisms due to sulfate-based stratospheric aerosol injection (SAI), a method of solar geoengineering. Using the GEOS-Chem atmospheric chemistry model, we determine the impact of SAI on tropospheric chemistry, starting with the impacts on stratospheric aerosol optical depth (AOD) and ozone. Arrows show the direction of causal relationships. Red indicates an increase in tropospheric mean concentration or rate of reaction and blue a decrease. Bold text indicates chemical changes that directly influence radiative forcing. Numbers in parenthesis indicate the resulting global mean percentage changes for key atmospheric species. Figure S1 in Supporting Information S1 presents a more detailed diagram.

nitrogen-saturated conditions (Rodhe et al., 2002), as the acidifying effects of nitrate and ammonium depend upon the biotic demand for nitrogen within an ecosystem, with nitrogen-limited systems readily taking up these two species. We exclude the flux of carboxylic acids, which are rapidly consumed by bacteria in soils or fresh water, and HCO_3^- , which is controlled by ambient CO_2 concentrations.

3. Results

We use the GEOS-Chem chemistry transport model to isolate the atmospheric photochemical response to a sulfate SAI scenario and to identify important chemical mechanisms (Eastham, Long, et al., 2018; Tilmes et al., 2015). Chemistry in the model is affected by SAI-induced changes in radiative flux in the UV and visible wavelengths, while meteorology and emissions remain the same. Key outcomes of the simulations are shown in Figure 1; Figure S1 in Supporting Information S1. We first summarize these outcomes (Sections 3.1–3.3) and then describe the driving mechanisms (Section 3.4).

3.1. Effects on Tropospheric Composition

Under SAI, the global annual mean tropospheric abundance of hydroxyl radical ($\text{OH}\cdot$) increases by 9%, enhancing the oxidative capacity of the atmosphere (Figures S2 and S3 in Supporting Information S1). Non- CO_2 greenhouse gases—methane, tropospheric ozone, and the halocarbons—mostly decline in the geoengineering scenario. In the troposphere, mean methane concentrations decline by $\sim 3.5\%$ (~ 60 ppb) (Figure S3 in Supporting Information S1), while the mean tropospheric ozone burden declines by 9% (~ 27 Tg). In the stratosphere, mean global methane decreases by 4% (~ 60 ppb) and the ozone burden by 11% (~ 327 Tg; Figure S3 in Supporting Information S1). Long-lived halocarbon concentrations in the stratosphere also decrease—for example, CFC-11 by 1% (1 ppt), HCFC-22 by 1% (0.6 ppt), and CCl_4 by 2% (0.5 ppt). Shorter-lived halocarbons decrease in both the troposphere and stratosphere—for example, HCFC-123 by $\sim 66\%$. At the surface, global mean ozone decreases

Impact of SAI chemical feedbacks on radiative forcing

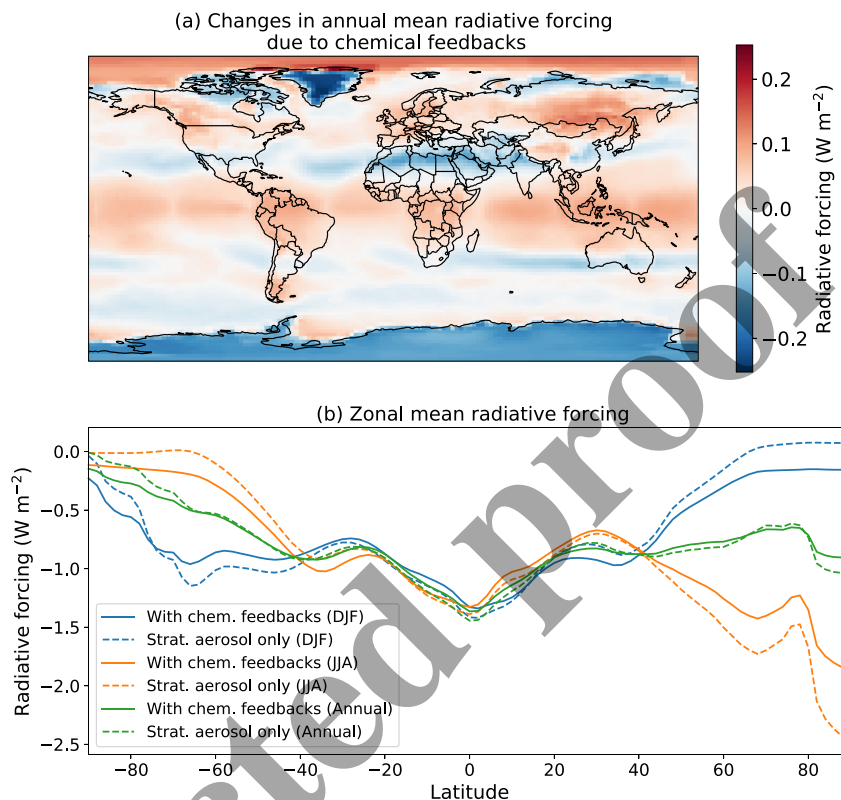


Figure 2. Impact of long-term chemical feedbacks from sulfate-based stratospheric aerosol injection (SAI) on radiative forcing. Panel (a) shows the change to SAI annual mean radiative forcing due to these chemical feedbacks. Panels (b) shows zonal mean radiative forcings from SAI without consideration of chemical feedbacks as dashed lines and with these feedbacks as solid lines, averaged over December-January-February (blue) and June-July-August (orange) and the whole year (green), as a function of latitude. Radiative forcings are instantaneous, calculated at the tropopause without stratospheric adjustment.

with geoengineering by $\sim 7\%$ (1.6 ppb; Figure S4 in Supporting Information S1). Surface concentrations of fine particulate matter ($PM_{2.5}$) are relatively unchanged in the global mean, but exhibit regional changes in the range of $\pm 1.5\%$ (Figure S4 in Supporting Information S1).

3.2. Radiative Forcing Effects

Not counting chemical feedbacks, the instantaneous radiative forcing at the tropopause from SAI is -0.92 W m^{-2} in the shortwave and $+0.12 \text{ W m}^{-2}$ in the longwave, for a net of -0.80 W m^{-2} . This is within the range of radiative forcing seen for simulations using the type of SAI scenario used here when chemical feedbacks are not included (Pitari et al., 2014; Tilmes et al., 2015) and within the range of radiative forcing efficiency for sulfur injections seen across various scenarios (Szopa et al., 2021). We find that the change in net forcing due to SAI-induced chemical feedbacks is negligible as a global annual mean ($+0.002 \text{ W m}^{-2}$, Figure 2). However, this small net change masks large shifts in the wavelength, spatial distribution, and seasonality of SAI forcing (Figure 2). For example, chemical feedbacks alone decrease the global mean annual forcing in the longwave by -0.24 W m^{-2} , which is compensated by increased shortwave forcing of $+0.24 \text{ W m}^{-2}$ (Figure S5 in Supporting Information S1).

The positive longwave forcing from SAI is due to absorption of terrestrial radiation by the added stratospheric aerosols (Kleinschmitt et al., 2018). Inclusion of chemical feedbacks counteracts this forcing due to the declines in the greenhouse gases methane, tropospheric ozone, and halocarbons, as described above. In contrast, in the shortwave, chemical feedbacks lead to warming attributable primarily to the decline in stratospheric ozone concentrations, which allows more UV sunlight to reach the Earth's surface. Over high albedo surfaces, such as Greenland and Antarctica, this warming effect is muted (Figure S5 in Supporting Information S1) due to the importance

of tropospheric ozone for radiative balance over high albedo surfaces (Mickley et al., 1999). With inclusion of chemical feedbacks, the SAI radiative forcing thus decreases 25% in the shortwave to become -0.69 W m^{-2} and changes sign in the longwave to become -0.11 W m^{-2} . The total radiative forcing including chemical feedbacks remains the same as without such feedbacks at -0.80 W m^{-2} , but the radiative effect of SAI has partially shifted from the shortwave to the longwave.

Because longwave radiation plays a larger role in the radiative balance in winter and shortwave in summer, these shifts in the wavelengths of radiative forcing resulting from chemical feedbacks have implications for the seasonal response of the climate to SAI. At a global mean level, chemical feedbacks increase the radiative effectiveness of geoengineering by $\sim 5\%$ in December-January-February and decrease the effectiveness in June-July-August also by 5% . Over the tropics, chemical feedbacks reduce the negative radiative forcing impact of geoengineering by $\sim 4\%$ year-round. Over mid latitudes, chemical feedbacks decrease the summertime decline in radiative forcing from geoengineering by $\sim 10\%$ but enhance the wintertime effect by $\sim 20\%$. Over northern high latitudes in summer, the effect is even greater: chemical feedbacks reduce negative radiative forcing from SAI there by $\sim 20\%$ at that time of year. In winter at these latitudes, chemical feedbacks flip the sign of SAI forcing from a slight positive to a negative forcing of -0.16 W m^{-2} . In contrast, for the southern high latitudes, chemical feedbacks increase the negative forcing effect year-round, by $\sim 16\%$ in summer and from near zero to -0.15 W m^{-2} in winter (Figure 2; Figure S5 and Table S1 in Supporting Information S1).

3.3. Effects on Public Health, Primary Production, Crop Yields, and Acid Deposition

When chemical feedbacks to SAI are considered, the changes in atmospheric composition changes lead to a decline in net global mortality of 60,000 (95% CI: 33,000 to 86,000) deaths per year (Figure 3, Data Set S1). Decreases in exposure to tropospheric ozone drive the net decline in mortality, with 67,000 (95% CI: 49,000 to 85,000) deaths avoided per year. This decline is partially offset by the additional premature deaths each year from increased $\text{PM}_{2.5}$ exposure in populous regions such as India (6,400 deaths globally, 95% CI: $-1,900$ to 14,000) and from increased UV exposure (1,000 deaths, 95% CI: 400 to 1,500; Figure S6 in Supporting Information S1 and Data Set S1).

Inclusion of chemical feedbacks in SAI enhances global total terrestrial GPP by $0.43 \text{ Gt C yr}^{-1}$, a $\sim 0.2\%$ increase (Figure 3), with the effects concentrated in the central and eastern United States, eastern Europe, India, and China, where the increases range from $\sim 1\%$ – 4% . Global staple crop production increases by $0.6 \times 10^{14} \text{ kcal yr}^{-1}$ ($\sim 1\%$), with crop yields increasing by over 10% in multiple regions in the northern midlatitudes (Figure 3). About two thirds of this increase in global crop yield is due to enhanced yield of wheat, the crop most sensitive to ozone. Global wheat yield increases by $3.6 \times 10^{13} \text{ kcal yr}^{-1}$ (11 Mton yr^{-1} , 2% ; Figure S7 in Supporting Information S1). The changes in GPP and crop yields simulated here can be traced to the decline in surface ozone, which damages vegetation. Prior studies of the impact of SAI on terrestrial GPP and crop yields, none of which have included the impact of changes in surface ozone but rather focused on changes in climate and radiation available for photosynthesis, have large disagreements in the magnitude and sometimes sign of the impact. Available estimates for the impact of SAI on terrestrial GPP range from a 3.8 Gt C yr^{-1} increase to a $14.7 \text{ Gt C yr}^{-1}$ decrease (Duan et al., 2020; Xia et al., 2016; Yang et al., 2020), and from a $\sim 0\%$ change to $\sim 10\%$ increase for the impact on global crop yields (Fan et al., 2021; Proctor et al., 2018). With regards to acid rain and acid deposition, we find minimal net changes due to chemical feedbacks.

3.4. Driving Chemical Mechanisms

The impacts of sulfate SAI on atmospheric chemical composition are driven by two competing effects on incoming solar radiation that vary with latitude: (a) increases in stratospheric aerosol optical depth (AOD) and (b) decreases in stratospheric ozone due to heterogeneous chemistry on stratospheric aerosols and increased photolysis. SAI increases simulated stratospheric AOD by factors of ~ 12.5 in the tropics and ~ 4.5 in high latitudes. Total column ozone, a key absorber of UV radiation, decreases by $\sim 15\%$ in high latitudes but only $\sim 5\%$ in the tropics (Figure S8 in Supporting Information S1). These levels of column ozone change from SAI are within the range of those seen in other studies using the GeoMIP G4 scenario (Pitari et al., 2014). The opposite pattern for changes in AOD and column ozone is also typical of tropical injection SAI scenarios such as the one used here and is primarily due to enhanced heterogeneous chemistry increasing ClO_x - and HO_x -catalyzed stratospheric ozone loss but decreasing

Impacts of SAI induced chemical changes on public health, GPP, and crop yields

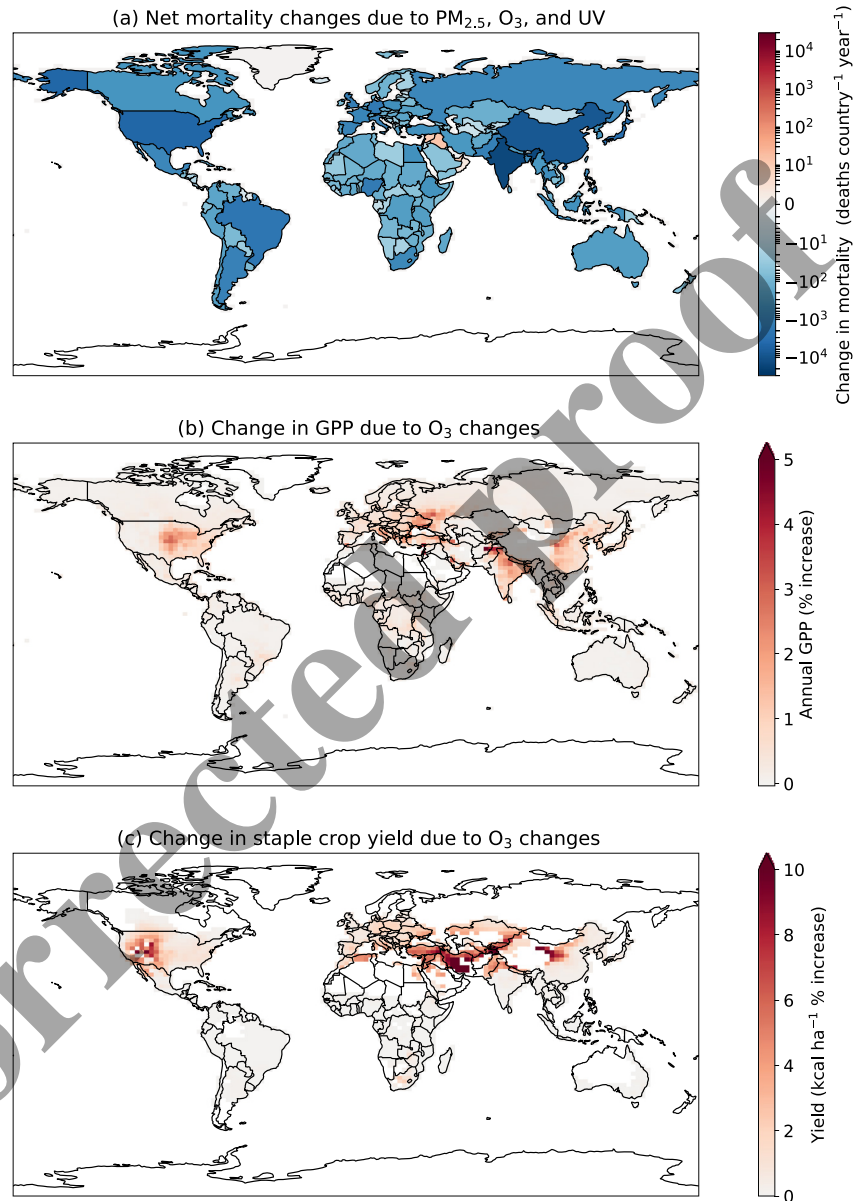


Figure 3. Impacts of atmospheric composition changes due to SAI geoengineering. (a) Net impact on premature mortality due to exposure to surface ozone, PM_{2.5}, and surface ultraviolet radiation, given the population in 2016. (b) Impact on terrestrial gross primary productivity (GPP) due to changes in surface ozone concentrations, expressed as the ratio between the simulations with and without geoengineering. Some regions show negligible (<0.5%) increase in GPP. (c) Effect on staple crop yield, again due to changing surface ozone, using 2016 base yields. The panel shows the sum of the changes in yield for wheat, maize, soybeans, and rice, normalized by equivalent food energy.

losses from NO_x, resulting in greater depletion at higher latitudes where ClO_x and HO_x are more important to the ozone budget (Pitari et al., 2014; Xia et al., 2017; Weisenstein et al., 2022; Figure S3 in Supporting Information S1). As a result of increased AOD, less total shortwave (~400–850 nm) radiation penetrates the tropopause and reaches the surface. In contrast, the loss of stratospheric ozone (Figure S3 in Supporting Information S1) allows more UV radiation at wavelengths shorter than ~345 nm to enter the troposphere, with UV reaching the surface increasing by ~1.6%. This UV increase is highest at high latitudes and lowest in the tropics (Figure S8 in Supporting Information S1).

The greater UV flux into the troposphere enhances the photolysis rate of tropospheric ozone to form $O(^1D)$ by $\sim 20\%$ on a global average (Figure S2 in Supporting Information S1). This increase in ozone photolysis is the main cause of the modeled decline in tropospheric ozone. It also drives the 9% increase in global mean tropospheric OH, a product of ozone photolysis, with increases ranging from $\sim 4\%$ – 5% in the tropics to $\sim 9\%$ – 16% over high latitudes (Figure S2 in Supporting Information S1). At the same time the rate of NO_2 photolysis, the primary driver of tropospheric ozone production, decreases globally by $\sim 1\%$ – 2% due to the decline in radiation in the near UV and visible wavelengths (i.e., wavelengths $> \sim 345$ nm) reaching the troposphere (Figures S2 and S8 in Supporting Information S1). The increases in UV at shorter wavelengths also result in a $\sim 40\%$ increase in the tropospheric photolysis rates for most halocarbon species.

The change in atmospheric oxidative capacity driven by increased OH has a cascading effect on atmospheric composition, including on the concentrations of greenhouse gases and surface air pollutants. Reaction with OH is the main sink of methane, and we estimate that the change in global mean OH reduces the methane lifetime against chemical removal by $\sim 8\%$. The decline in methane also feeds back on the concentration of OH (Szopa et al., 2021). Under geoengineering, these long-term interactions between OH and methane tend to increase OH and reduce methane until a new chemical equilibrium is reached.

For NO_x (defined here as $NO + NO_2$), various competing processes result in a mean tropospheric increase of ~ 1 ppt in the geoengineering scenario. To begin with, the daytime reaction of NO_x to form HNO_3 increases under SAI due to higher OH levels. At night, NO_x oxidation to HNO_3 decreases due to lower ozone levels, which reduces formation of NO_3 and N_2O_5 . The decrease in the nighttime sink appears to dominate globally, as the spatial pattern of increased NO_x for the midlatitudes corresponds to those regions where NO_3 and N_2O_5 levels decline (Figure S9 in Supporting Information S1).

As with NO_x , perturbations to $PM_{2.5}$ in the geoengineering scenario can be traced to several counteracting effects. Surface sulfate concentrations increase by $\sim 1\%$ – 3% in the high latitudes and mid-latitudes, while decreasing by $\sim 0.5\%$ – 2% in the tropics (Figure S10 in Supporting Information S1). The main driver for the enhancement in sulfate here is an increase in gas-phase oxidation of SO_2 by OH. The increases in sulfate production rates are partially compensated by a $\sim 2\%$ – 4% decrease in in-cloud oxidation of SO_2 by ozone.

Total mean nitrate (particulate and gaseous) decreases in the mid latitudes but increases in the tropics (Figure S9 in Supporting Information S1). The decreases in particulate nitrate mostly occur where sulfate increases (Figure S10 in Supporting Information S1), suggesting ammonia-limited conditions where each additional sulfate anion in a particle displaces two nitrate anions. Ammonium shows small enhancements in regions where $PM_{2.5}$ is not entirely ammonia-limited, but it decreases slightly in the northern midlatitudes, corresponding to the changes in total nitrate (Figures S9 and S10 in Supporting Information S1). Organic aerosol increases slightly in many regions, reflecting faster oxidation of SOA precursors due to enhanced OH (Figure S10 in Supporting Information S1). Given the relatively simple SOA scheme in our simulations, however, the response of SOA to geoengineering in our model is muted (39).

4. Conclusions and Implications

We find that long-term chemical feedbacks increase the atmospheric oxidative capacity with regard to OH and alter the radiative forcing from sulfate-based SAI. These results point to important gaps in prior studies of the impacts of geoengineering, especially with regards to those impacts on regional and seasonal scales (Dai et al., 2018; Irvine & Keith, 2020; Kravitz et al., 2017; Kravitz et al., 2021; MacMartin et al., 2017; Tilmes et al., 2018; Xu et al., 2020). In particular, the 10%–20% decline in negative radiative forcing during hemispheric summer over the southern midlatitudes and the northern mid- and high latitudes implies that SAI could be less effective than anticipated at reducing summer heat waves or preserving Arctic summer sea ice. At the same time, the enhanced negative radiative forcing over southern high latitudes year-round and during winter for mid latitudes implies that SAI might be more effective than expected for maintaining the Antarctic ice sheet or preserving midlatitude winter snowfall. Our results thus imply that geoengineering studies aiming to optimize climate at regional levels (Dai et al., 2018; Kravitz et al., 2016; MacMartin et al., 2017) may include substantial errors due to neglect of chemical feedbacks and the resulting changes in concentrations of greenhouse gases like methane and tropospheric ozone. Consideration of chemical feedbacks would also likely alter estimates of the impacts of geoengineering on crops, vegetation, and ecosystem health (Dagon & Schrag, 2019; Fan et al., 2021;

Proctor et al., 2018; Visioni et al., 2020), with such feedbacks increasing crop yield and GPP, and potentially canceling out the deleterious effects of additional sulfur on acid precipitation and deposition.

Because SAI has not been implemented and volcanic eruptions are imperfect analogs for SAI, there is no direct observational evidence that could support the chemical changes simulated here. Nevertheless, studies of the impact of the 1992 Mt. Pinatubo eruption do provide some circumstantial observational support for the idea that SAI and stratospheric ozone depletion increase atmospheric oxidative capacity. Multiple studies observed anomalous declines in surface and tropospheric ozone following the Mt. Pinatubo eruption that are consistent with increased ozone photolysis due to heightened stratospheric ozone depletion (Fusco & Logan, 2003; Harris & Oltmans, 1997; Lin et al., 2015; Oltmans et al., 1998). Also consistent with the chemical mechanisms identified here is the observed slowdown in the growth rate of atmospheric methane following the Pinatubo eruption, which previous studies have suggested may have been driven in part by increases in atmospheric oxidative capacity resulting from stratospheric ozone depletion (Bândă et al., 2013, 2016; Bekki et al., 1994).

Anthropogenic climate change has been estimated to reduce global mean surface ozone by ~ 0.55 ppb for each 0.5°C increment of additional warming (Szopa et al., 2021). Given the temperature change that might be expected from the type of SAI scenario used here (Xia et al., 2016, 2017), our results suggest that the photochemical effects on surface ozone might be more than twice as large as temperature-driven ones. The limited observational evidence from the Pinatubo eruption also suggests a dominant role for the photochemical response to SAI in determining atmospheric composition changes. However, there remain various uncertainties, related to chemistry and to other aspects of the Earth System, that will require the use of a detailed coupled chemistry-climate model or full Earth System model to further investigate. For example, SAI induced changes in the hydrological cycle could affect both OH production and cloud chemistry rates, all with implications for the net radiative response (Tilmes et al., 2013; Visioni et al., 2017). Other examples include the impacts of SAI on ecosystems and biogenic VOC emissions (Duan et al., 2020; Telford et al., 2010; Xia et al., 2016; Yang et al., 2020) and on stratospheric water vapor. The use of a coupled chemistry-climate model or full Earth System model is also needed to fully characterize the relationship between changes to instantaneous radiative forcing from SAI and the associated chemical feedbacks and ultimate climate response (Szopa et al., 2021).

A key uncertainty arising from inclusion of chemical feedbacks is that the net radiative forcing from geoengineering may depend on the background atmospheric composition. For example, in a world where surface SO_2 emissions have significantly declined, geoengineering could increase concentrations of $\text{PM}_{2.5}$ since the SAI-induced increases in nitrate would not be compensated by changes in sulfate. Chemical feedbacks thus add an additional layer of complexity to using geoengineering to maintain a stable climate while buying time for emissions reductions (Irvine & Keith, 2020; Irvine et al., 2016; Keith & MacMartin, 2015), since the radiative forcing derived from a constant intervention can change over time due to surface emissions.

Counterintuitively, our analysis shows that the decline in stratospheric ozone from injection of sulfate aerosol may lead to some beneficial side effects, including a net decrease in mortality and a decline in some tropospheric greenhouse gases. Our work suggests that other geoengineering strategies such as calcite aerosol injection or deployment of space mirrors (Keith et al., 2016; Kravitz et al., 2021) could increase concentrations of greenhouse gases, reducing the net cooling. In contrast to sulfate injection, these other strategies would cut shortwave radiation at all wavelengths in the troposphere, decreasing OH \cdot , the main sink of methane, and slowing photolysis of halocarbons and tropospheric ozone. These strategies may also lead to increases in global mortality, as increased mortality from higher surface ozone levels would likely outweigh declines in mortality due to decreases in UV radiation exposure.

The identified linkages between stratospheric ozone depletion and surface air quality also have implications for the Montreal Protocol, the international agreement which governs the production and consumption of ozone depleting substances with the aim of protecting human health and the environment. Given SAI induced stratospheric ozone depletion starting at near present-day conditions, our results suggest a roughly 60 to 1 ratio for reduced mortality from surface air pollution changes compared to increased mortality from UV exposure. Since SAI also reduces near-UV radiation and NO_2 photolysis, a sulfate SAI scenario likely results in a slightly larger surface ozone decline than would be expected from an equivalent loss of stratospheric ozone due to emissions of ozone depleting substances such as CFCs. In any event, multiple studies have nevertheless demonstrated a positive correlation between stratospheric and tropospheric ozone levels, implying increases in surface ozone as the

stratospheric ozone layer recovers (Eastham, Keith, et al., 2018; Hodzic & Madronich, 2018; Isaksen et al., 2005; WMO, 2022; Zeng et al., 2010; Zhang et al., 2014).

Although our work does not consider the effects of SAI-induced changes to meteorology on atmospheric composition, it nevertheless demonstrates the importance of atmospheric chemistry to the impact of geoengineering. Without considering long-term chemical feedbacks, estimates of the climate effects of geoengineering may embody significant errors, especially with regards to the seasonal and spatial pattern of radiative forcing. Our analysis suggests that deploying geoengineering methods designed to avoid stratospheric ozone depletion may be counterproductive for climate and public health goals. The complexity of the climate system and the possibility of unexpected “surprises” is often pointed to as a reason for caution when considering geoengineering as a means to mitigate the harms resulting from climate change (Kravitz & MacMartin, 2020; Robock, 2020). Given that the geoengineering research community has not previously identified long-term chemical feedbacks as a key uncertainty (Lee et al., 2021; National Academies of Sciences, Engineering, and Medicine, 2021; Patt et al., 2022), this work reveals just such a “surprise” with respect to prior studies.

Conflict of Interest

The authors declare no conflicts of interest relevant to this study.

Data Availability Statement

Model output, including Data Set S1, is available at: <https://doi.org/10.7910/DVN/ZWVSWC>. GEOS-Chem version 13.0.0 code with RRTMG is available at: <https://doi.org/10.5281/zenodo.4429193>. TEMIR code is available at: <https://doi.org/10.5281/zenodo.6380767>.

References

- Alexander, B., Allman, D. J., Amos, H. M., Fairlie, T. D., Dachs, J., Hegg, D. A., & Sletten, R. S. (2012). Isotopic constraints on the formation pathways of sulfate aerosol in the marine boundary layer of the subtropical northeast Atlantic Ocean. *Journal of Geophysical Research*, 117(D6), D06304. <https://doi.org/10.1029/2011JD016773>
- Alexander, B., & Mickley, L. J. (2015). Paleo-perspectives on potential future changes in the oxidative capacity of the atmosphere due to climate change and anthropogenic emissions. *Current Pollution Reports*, 1(2), 57–69. <https://doi.org/10.1007/s40726-015-0006-0>
- Aquila, V., Oman, L. D., Stolarski, R. S., Colarco, P. R., & Newman, P. A. (2012). Dispersion of the volcanic sulfate cloud from a Mount Pinatubo-like eruption. *Journal of Geophysical Research*, 117(D6), D06216. <https://doi.org/10.1029/2011JD016968>
- Bändä, N., Krol, M., van Weele, M., van Noije, T., Le Sager, P., & Röckmann, T. (2016). Can we explain the observed methane variability after the Mount Pinatubo eruption? *Atmospheric Chemistry and Physics*, 16(1), 195–214. <https://doi.org/10.5194/acp-16-195-2016>
- Bändä, N., Krol, M., van Weele, M., van Noije, T., & Röckmann, T. (2013). Analysis of global methane changes after the 1991 Pinatubo volcanic eruption. *Atmospheric Chemistry and Physics*, 13(4), 2267–2281. <https://doi.org/10.5194/acp-13-2267-2013>
- Bekki, S., Law, K. S., & Pyle, J. A. (1994). Effect of ozone depletion on atmospheric CH₄ and CO concentrations. *Nature*, 371(6498), 595–597. <https://doi.org/10.1038/371595a0>
- Bian, H., & Prather, M. J. (2002). Fast-J2: Accurate simulation of stratospheric photolysis in global chemical models. *Journal of Atmospheric Chemistry*, 41(3), 281–296. <https://doi.org/10.1023/A:1014980619462>
- Center for International Earth Science Information Network—CIESIN—Columbia University. (2018). *Gridded population of the world, version 4.11 (GPWv4)*. NASA Socioeconomic Data and Applications Center (SEDAC). <https://doi.org/10.7927/H4JW8BX5>
- Crutzen, P. J. (2006). Albedo enhancement by stratospheric sulfur injections: A contribution to resolve a policy dilemma? *Climatic Change*, 77(3), 211. <https://doi.org/10.1007/s10584-006-9101-y>
- Dagon, K., & Schrag, D. P. (2019). Quantifying the effects of solar geoengineering on vegetation. *Climatic Change*, 153(1), 235–251. <https://doi.org/10.1007/s10584-019-02387-9>
- Dai, Z., Weisenstein, D. K., & Keith, D. W. (2018). Tailoring meridional and seasonal radiative forcing by sulfate aerosol solar geoengineering. *Geophysical Research Letters*, 45(2), 1030–1039. <https://doi.org/10.1002/2017GL076472>
- Duan, L., Cao, L., Bala, G., & Caldeira, K. (2019). Climate response to pulse versus sustained stratospheric aerosol forcing. *Geophysical Research Letters*, 46(15), 8976–8984. <https://doi.org/10.1029/2019GL083701>
- Duan, L., Cao, L., Bala, G., & Caldeira, K. (2020). A model-based investigation of terrestrial plant carbon uptake response to four radiation modification approaches. *Journal of Geophysical Research: Atmospheres*, 125(9), e2019JD031883. <https://doi.org/10.1029/2019JD031883>
- Eastham, S. D., Keith, D. W., & Barrett, S. R. H. (2018). Mortality tradeoff between air quality and skin cancer from changes in stratospheric ozone. *Environmental Research Letters*, 13(3), 034035. <https://doi.org/10.1088/1748-9326/aaad2e>
- Eastham, S. D., Long, M. S., Keller, C. A., Lundgren, E., Yantosca, R. M., Zhuang, J., et al. (2018). GEOS-Chem high performance (GCHP v11-02c): A next-generation implementation of the GEOS-Chem chemical transport model for massively parallel applications. *Geoscientific Model Development*, 11(7), 2941–2953. <https://doi.org/10.5194/gmd-11-2941-2018>
- Eastham, S. D., Weisenstein, D. K., & Barrett, S. R. H. (2014). Development and evaluation of the unified tropospheric–stratospheric chemistry extension (UCX) for the global chemistry–transport model GEOS-Chem. *Atmospheric Environment*, 89, 52–63. <https://doi.org/10.1016/j.atmosenv.2014.02.001>
- Eastham, S. D., Weisenstein, D. K., Keith, D. W., & Barrett, S. R. H. (2018). Quantifying the impact of sulfate geoengineering on mortality from air quality and UV-B exposure. *Atmospheric Environment*, 187, 424–434. <https://doi.org/10.1016/j.atmosenv.2018.05.047>

Acknowledgments

The authors thank the GeoMIP project for providing the aerosol fields associated with the G4-SSA model experiment. The GEOS-FP meteorological data used in this study have been provided by the Global Modeling and Assimilation Office (GMAO) at NASA Goddard Space Flight Center. This work was supported by the Harvard University Solar Geoengineering Research Program. Any opinions and conclusions expressed herein are those of the authors and do not necessarily reflect the views or policies of the US Government. This work was primarily completed while Dr. Moch was at Harvard University.

- Fan, Y., Tjiputra, J., Muri, H., Lombardozi, D., Park, C.-E., Wu, S., & Keith, D. (2021). Solar geoengineering can alleviate climate change pressures on crop yields. *Nature Food*, 2(5), 373–381. <https://doi.org/10.1038/s43016-021-00278-w>
- Fusco, A. C., & Logan, J. A. (2003). Analysis of 1970–1995 trends in tropospheric ozone at Northern Hemisphere midlatitudes with the GEOS-CHEM model. *Journal of Geophysical Research*, 108(D15), 4449. <https://doi.org/10.1029/2002JD002742>
- Guenther, A. B., Jiang, X., Heald, C. L., Sakulyanontvittaya, T., Duhl, T., Emmons, L. K., & Wang, X. (2012). The model of emissions of gases and aerosols from nature version 2.1 (MEGAN2.1): An extended and updated framework for modeling biogenic emissions. *Geoscientific Model Development*, 5(6), 1471–1492. <https://doi.org/10.5194/gmd-5-1471-2012>
- Harris, J. M., & Oltmans, S. J. (1997). Variations in tropospheric ozone related to transport at American Samoa. *Journal of Geophysical Research*, 102(D7), 8781–8791. <https://doi.org/10.1029/97JD00238>
- Heald, C. L., Ridley, D. A., Kroll, J. H., Barrett, S. R. H., Cady-Pereira, K. E., Alvarado, M. J., & Holmes, C. D. (2014). Contrasting the direct radiative effect and direct radiative forcing of aerosols. *Atmospheric Chemistry and Physics*, 14(11), 5513–5527. <https://doi.org/10.5194/acp-14-5513-2014>
- Hodzic, A., & Madronich, S. (2018). Response of surface ozone over the continental United States to UV radiation declines from the expected recovery of stratospheric ozone. *Npj Climate and Atmospheric Science*, 1(1), 1–7. <https://doi.org/10.1038/s41612-018-0045-5>
- Iacono, M. J., Delamere, J. S., Mlawer, E. J., Shephard, M. W., Clough, S. A., & Collins, W. D. (2008). Radiative forcing by long-lived greenhouse gases: Calculations with the AER radiative transfer models. *Journal of Geophysical Research*, 113(D13), D13103. <https://doi.org/10.1029/2008JD009944>
- Iizumi, T., & Sakai, T. (2020). The global dataset of historical yields for major crops 1981–2016. *Scientific Data*, 7(1), 97. <https://doi.org/10.1038/s41597-020-0433-7>
- Irvine, P., Emanuel, K., He, J., Horowitz, L. W., Vecchi, G., & Keith, D. (2019). Halving warming with idealized solar geoengineering moderates key climate hazards. *Nature Climate Change*, 9(4), 295–299. <https://doi.org/10.1038/s41558-019-0398-8>
- Irvine, P. J., & Keith, D. W. (2020). Halving warming with stratospheric aerosol geoengineering moderates policy-relevant climate hazards. *Environmental Research Letters*, 15(4), 044011. <https://doi.org/10.1088/1748-9326/ab76de>
- Irvine, P. J., Kravitz, B., Lawrence, M. G., & Muri, H. (2016). An overview of the Earth system science of solar geoengineering. *WIREs Climate Change*, 7(6), 815–833. <https://doi.org/10.1002/wcc.423>
- Isaksen, I. S. A., Zerefos, C., Kourtidis, K., Meleti, C., Dalsøren, S. B., Sundet, J. K., et al. (2005). Tropospheric ozone changes at unpolluted and semipolluted regions induced by stratospheric ozone changes. *Journal of Geophysical Research*, 110(D2), D02302. <https://doi.org/10.1029/2004JD004618>
- Jacob, D. J. (2000). Heterogeneous chemistry and tropospheric ozone. *Atmospheric Environment*, 34(12), 2131–2159. [https://doi.org/10.1016/S1352-2310\(99\)00462-8](https://doi.org/10.1016/S1352-2310(99)00462-8)
- Jerrett, M., Burnett, R. T., Pope, C. A., Ito, K., Thurston, G., Krewski, D., et al. (2009). Long-term ozone exposure and mortality. *New England Journal of Medicine*, 360(11), 1085–1095. <https://doi.org/10.1056/NEJMoa0803894>
- Keith, D. W., & Irvine, P. J. (2016). Solar geoengineering could substantially reduce climate risks—A research hypothesis for the next decade. *Earth's Future*, 4(11), 549–559. <https://doi.org/10.1002/2016EF000465>
- Keith, D. W., & MacMartin, D. G. (2015). A temporary, moderate and responsive scenario for solar geoengineering. *Nature Climate Change*, 5(3), 201–206. <https://doi.org/10.1038/nclimate2493>
- Keith, D. W., Weisenstein, D. K., Dykema, J. A., & Keutsch, F. N. (2016). Stratospheric solar geoengineering without ozone loss. *Proceedings of the National Academy of Sciences of the United States of America*, 113(52), 14910–14914. <https://doi.org/10.1073/pnas.1615572113>
- Kleinschmitt, C., Boucher, O., & Platt, U. (2018). Sensitivity of the radiative forcing by stratospheric sulfur geoengineering to the amount and strategy of the SO₂ injection studied with the LMDZ-S3A model. *Atmospheric Chemistry and Physics*, 18(4), 2769–2786. <https://doi.org/10.5194/acp-18-2769-2018>
- Kravitz, B., & MacMartin, D. G. (2020). Uncertainty and the basis for confidence in solar geoengineering research. *Nature Reviews Earth & Environment*, 1(1), 64–75. <https://doi.org/10.1038/s43017-019-0004-7>
- Kravitz, B., MacMartin, D. G., Mills, M. J., Richter, J. H., Tilmes, S., Lamarque, J.-F., et al. (2017). First simulations of designing stratospheric sulfate aerosol geoengineering to meet multiple simultaneous climate objectives. *Journal of Geophysical Research: Atmospheres*, 122(23), 12616–12634. <https://doi.org/10.1002/2017JD026874>
- Kravitz, B., MacMartin, D. G., Vioni, D., Boucher, O., Cole, J. N. S., Haywood, J., et al. (2021). Comparing different generations of idealized solar geoengineering simulations in the Geoengineering Model Intercomparison Project (GeoMIP). *Atmospheric Chemistry and Physics*, 21(6), 4231–4247. <https://doi.org/10.5194/acp-21-4231-2021>
- Kravitz, B., MacMartin, D. G., Wang, H., & Rasch, P. J. (2016). Geoengineering as a design problem. *Earth System Dynamics*, 7(2), 469–497. <https://doi.org/10.5194/esd-7-469-2016>
- Kravitz, B., Robock, A., Boucher, O., Schmidt, H., Taylor, K. E., Stenchikov, G., & Schulz, M. (2011). The Geoengineering Model Intercomparison Project (GeoMIP). *Atmospheric Science Letters*, 12(2), 162–167. <https://doi.org/10.1002/asl.316>
- Lee, J.-Y., Marotzke, J., Bala, G., Cao, L., Corti, S., Dunne, J. P., et al. (2021). Future global climate: Scenario-based projections and near-term information. In V. Masson-Delmotte, P. Zhai, A. Pirani, S. L. Connors, C. Péan, S. Berger, et al. (Eds.), *Climate change 2021: The physical science basis. Contribution of working group I to the sixth assessment report of the intergovernmental panel on climate change* (pp. 553–672). Cambridge University Press. <https://doi.org/10.1017/9781009157896.006>
- Lin, M., Fiore, A. M., Horowitz, L. W., Langford, A. O., Oltmans, S. J., Tarasick, D., & Rieder, H. E. (2015). Climate variability modulates western US ozone air quality in spring via deep stratospheric intrusions. *Nature Communications*, 6(1), 7105. <https://doi.org/10.1038/ncomms8105>
- MacMartin, D. G., Kravitz, B., Tilmes, S., Richter, J. H., Mills, M. J., Lamarque, J.-F., et al. (2017). The climate response to stratospheric aerosol geoengineering can be tailored using multiple injection locations. *Journal of Geophysical Research: Atmospheres*, 122(23), 12574–12590. <https://doi.org/10.1002/2017JD026868>
- Mao, J., Jacob, D. J., Evans, M. J., Olson, J. R., Ren, X., Brune, W. H., et al. (2010). Chemistry of hydrogen oxide radicals (HO_x) in the Arctic troposphere in spring. *Atmospheric Chemistry and Physics*, 10(13), 5823–5838. <https://doi.org/10.5194/acp-10-5823-2010>
- McCormick, M. P., Thomason, L. W., & Trepte, C. R. (1995). Atmospheric effects of the Mt Pinatubo eruption. *Nature*, 373(6513), 399–404. <https://doi.org/10.1038/373399a0>
- Mickley, L. J., Murti, P. P., Jacob, D. J., Logan, J. A., Koch, D. M., & Rind, D. (1999). Radiative forcing from tropospheric ozone calculated with a unified chemistry-climate model. *Journal of Geophysical Research*, 104(D23), 30153–30172. <https://doi.org/10.1029/1999JD900439>
- Mills, M. J., Richter, J. H., Tilmes, S., Kravitz, B., MacMartin, D. G., Glanville, A. A., et al. (2017). Radiative and chemical response to interactive stratospheric sulfate aerosols in fully coupled CESM1 (WACCM). *Journal of Geophysical Research: Atmospheres*, 122(23), 13061–13078. <https://doi.org/10.1002/2017JD027006>

- Moch, J. M., Dovrou, E., Mickley, L. J., Keutsch, F. N., Cheng, Y., Jacob, D. J., et al. (2018). Contribution of hydroxymethane sulfonate to ambient particulate matter: A potential explanation for high particulate sulfur during severe winter haze in Beijing. *Geophysical Research Letters*, 45(21), 11969–11979. <https://doi.org/10.1029/2018GL079309>
- Moch, J. M., Mickley, L. J., Eastham, S. D., Lundgren, E. W., Shah, V., Buonocore, J. J., et al. (2023). Overlooked long-term atmospheric chemical feedbacks alter the impact of solar geoengineering: Implications for tropospheric oxidative capacity (version 2.1) [Dataset]. Harvard Dataverse. <https://doi.org/10.7910/DVN/ZWVSWC>
- Murray, L. T. (2016). Lightning NO_x and impacts on air quality. *Current Pollution Reports*, 2(2), 115–133. <https://doi.org/10.1007/s40726-016-0031-7>
- National Academies of Sciences, Engineering & Medicine. (2021). *Reflecting sunlight: Recommendations for solar geoengineering research and research governance*. The National Academies Press. <https://doi.org/10.17226/25762>
- Oleson, K., Lawrence, M., Bonan, B., Drewniak, B., Huang, M., Koven, D., et al. (2013). Technical description of version 4.5 of the community land model (CLM). <https://doi.org/10.5065/D6RR1W7M>
- Oltmans, S. J., Lefohn, A. S., Scheel, H. E., Harris, J. M., Levy, H., II., Galbally, I. E., et al. (1998). Trends of ozone in the troposphere. *Geophysical Research Letters*, 25(2), 139–142. <https://doi.org/10.1029/97GL03505>
- Pai, S. J., Heald, C. L., Pierce, J. R., Farina, S. C., Marais, E. A., Jimenez, J. L., et al. (2020). An evaluation of global organic aerosol schemes using airborne observations. *Atmospheric Chemistry and Physics*, 20(5), 2637–2665. <https://doi.org/10.5194/acp-20-2637-2020>
- Park, R. J., Jacob, D. J., Field, B. D., Yantosca, R. M., & Chin, M. (2004). Natural and transboundary pollution influences on sulfate-nitrate-ammonium aerosols in the United States: Implications for policy. *Journal of Geophysical Research*, 109(D15), D15204. <https://doi.org/10.1029/2003JD004473>
- Patt, A., Rajamani, L., Bhandari, P., Ivanova Boncheva, A., Caparrós, A., Djemouai, K., et al. (2022). International cooperation. In P. R. Shukla, J. Skea, R. Slade, A. Al Khourdajie, R. van Diemen, D. McCollum, et al. (Eds.), *IPCC, 2022: Climate change 2022: Mitigation of climate change. Contribution of working group III to the sixth assessment report of the intergovernmental panel on climate change*. Cambridge University Press. <https://doi.org/10.1017/9781009157926.016>
- Pitari, G., Aquila, V., Kravitz, B., Robock, A., Watanabe, S., Cionni, I., et al. (2014). Stratospheric ozone response to sulfate geoengineering: Results from the Geoengineering Model Intercomparison Project (GeoMIP). *Journal of Geophysical Research: Atmospheres*, 119(5), 2629–2653. <https://doi.org/10.1002/2013JD020566>
- Pitari, G., Mancini, E., Rizi, V., & Shindell, D. T. (2002). Impact of future climate and emission changes on stratospheric aerosols and ozone. *Journal of the Atmospheric Sciences*, 59(3), 414–440. [https://doi.org/10.1175/1520-0469\(2002\)059<0414:IOFCAE>2.0.CO;2](https://doi.org/10.1175/1520-0469(2002)059<0414:IOFCAE>2.0.CO;2)
- Proctor, J., Hsiang, S., Burney, J., Burke, M., & Schlenker, W. (2018). Estimating global agricultural effects of geoengineering using volcanic eruptions. *Nature*, 560(7719), 480–483. <https://doi.org/10.1038/s41586-018-0417-3>
- Rienecker, M., Suarez, M. J., Todling, R., Bacmeister, J., Takacs, L., Liu, H.-C., et al. (2008). The GEOS-5 data assimilation system—Documentation of versions 5.0.1, 5.1.0, and 5.2.0 (technical report). In *Series on global modeling and data assimilation* (Vol. 27). National Aeronautics and Space Administration. NASA/TM–2008–104606. Goddard Space Flight Center Greenbelt, Maryland 20771. Retrieved from <https://gmao.gsfc.nasa.gov/pubs/docs/tm27.pdf>
- Robock, A. (2020). Benefits and risks of stratospheric solar radiation management for climate intervention (geoengineering). *Bridge*, 50(1), 59–67.
- Rodhe, H., Dentener, F., & Schulz, M. (2002). The global distribution of acidifying wet deposition. *Environmental Science & Technology*, 36(20), 4382–4388. <https://doi.org/10.1021/es020057g>
- Sacks, W. J., Deryng, D., Foley, J. A., & Ramankutty, N. (2010). Crop planting dates: An analysis of global patterns. *Global Ecology and Biogeography*, 19(5), 607–620. <https://doi.org/10.1111/j.1466-8238.2010.00551.x>
- Schmidt, G. A., Ruedy, R., Hansen, J. E., Aleinov, I., Bell, N., Bauer, M., et al. (2006). Present-day atmospheric simulations using GISS ModelE: Comparison to in situ, satellite, and reanalysis data. *Journal of Climate*, 19(2), 153–192. <https://doi.org/10.1175/JCLI3612.1>
- Shah, V., Jacob, D. J., Moch, J. M., Wang, X., & Zhai, S. (2020). Global modeling of cloud water acidity, precipitation acidity, and acid inputs to ecosystems. *Atmospheric Chemistry and Physics*, 20(20), 12223–12245. <https://doi.org/10.5194/acp-20-12223-2020>
- Sherwen, T., Schmidt, J. A., Evans, M. J., Carpenter, L. J., Großmann, K., Eastham, S. D., et al. (2016). Global impacts of tropospheric halogens (Cl, Br, I) on oxidants and composition in GEOS-Chem. *Atmospheric Chemistry and Physics*, 16(18), 12239–12271. <https://doi.org/10.5194/acp-16-12239-2016>
- Sitch, S., Cox, P. M., Collins, W. J., & Huntingford, C. (2007). Indirect radiative forcing of climate change through ozone effects on the land-carbon sink. *Nature*, 448(7155), 791–794. <https://doi.org/10.1038/nature06059>
- Slaper, H., Velders, G. J. M., Daniel, J. S., de Grijl, F. R., & van der Leun, J. C. (1996). Estimates of ozone depletion and skin cancer incidence to examine the Vienna Convention achievements. *Nature*, 384(6606), 256–258. <https://doi.org/10.1038/384256a0>
- Szopa, S., Naik, V., Adhikary, B., Artaxo, P., Bernsten, T., Collins, W. D., et al. (2021). Short-lived climate forcers. In V. Masson-Delmotte, P. Zhai, A. Pirani, S. L. Connors, C. Péan, S. Berger, et al. (Eds.), *Climate change 2021: The physical science basis. Contribution of working group I to the sixth assessment report of the intergovernmental panel on climate change* (pp. 817–922). Cambridge University Press. <https://doi.org/10.1017/9781009157896.008>
- Tai, A. P. K., Martin, M. V., & Heald, C. L. (2014). Threat to future global food security from climate change and ozone air pollution. *Nature Climate Change*, 4(9), 817–821. <https://doi.org/10.1038/nclimate2317>
- Tai, A. P. K., Sadiq, M., Pang, J. Y. S., Yung, D. H. Y., & Feng, Z. (2021). Impacts of surface ozone pollution on global crop yields: Comparing different ozone exposure metrics and incorporating co-effects of CO₂. *Frontiers in Sustainable Food Systems*, 5. <https://doi.org/10.3389/fsufs.2021.534616>
- Tai, A. P. K., & Val Martin, M. (2017). Impacts of ozone air pollution and temperature extremes on crop yields: Spatial variability, adaptation and implications for future food security. *Atmospheric Environment*, 169, 11–21. <https://doi.org/10.1016/j.atmosenv.2017.09.002>
- Tai, A. P. K., & Yung, D. H. Y. (2022). Terrestrial ecosystem model in R [Software]. Zenodo. <https://doi.org/10.5281/zenodo.6380767>
- Tai, A. P. K., Yung, D. H. Y., & Lam, T. (2023). Terrestrial Ecosystem Model in R (TEMIR) version 1.0: Simulating ecophysiological responses of vegetation to atmospheric chemical and meteorological changes. *EGUsphere*, 1–46. <https://doi.org/10.5194/egusphere-2023-1287>
- Telford, P. J., Lathière, J., Abraham, N. L., Archibald, A. T., Braesicke, P., Johnson, C. E., et al. (2010). Effects of climate-induced changes in isoprene emissions after the eruption of Mount Pinatubo. *Atmospheric Chemistry and Physics*, 10(15), 7117–7125. <https://doi.org/10.5194/acp-10-7117-2010>
- The International GEOS-Chem User Community. (2021). Geoschem/GCHP 13.0.0-rc.0: GEOS-Chem 13.0.0 release candidate (in GCHP mode) (13.0.0-rc.0) [Software]. Zenodo. <https://doi.org/10.5281/zenodo.4429194>

- Tilmes, S., Fasullo, J., Lamarque, J.-F., Marsh, D. R., Mills, M., Alterskjær, K., et al. (2013). The hydrological impact of geoengineering in the Geoengineering Model Intercomparison Project (GeoMIP). *Journal of Geophysical Research: Atmospheres*, *118*(19), 11036–11058. <https://doi.org/10.1002/jgrd.50868>
- Tilmes, S., Garcia, R. R., Kinnison, D. E., Gettelman, A., & Rasch, P. J. (2009). Impact of geoengineered aerosols on the troposphere and stratosphere. *Journal of Geophysical Research*, *114*(D12), D12305. <https://doi.org/10.1029/2008JD011420>
- Tilmes, S., Mills, M. J., Niemeier, U., Schmidt, H., Robock, A., Kravitz, B., et al. (2015). A new Geoengineering Model Intercomparison Project (GeoMIP) experiment designed for climate and chemistry models. *Geoscientific Model Development*, *8*(1), 43–49. <https://doi.org/10.5194/gmd-8-43-2015>
- Tilmes, S., Richter, J. H., Kravitz, B., MacMartin, D. G., Mills, M. J., Simpson, I. R., et al. (2018). CESM1(WACCM) stratospheric aerosol geoengineering large ensemble project. *Bulletin of the American Meteorological Society*, *99*(11), 2361–2371. <https://doi.org/10.1175/BAMS-D-17-0267.1>
- Tracy, S. M., Moch, J. M., Eastham, S. D., & Buonocore, J. J. (2022). Stratospheric aerosol injection may impact global systems and human health outcomes. *Elementa: Science of the Anthropocene*, *10*(1), 00047. <https://doi.org/10.1525/elementa.2022.00047>
- Travis, K. R., Jacob, D. J., Fisher, J. A., Kim, P. S., Marais, E. A., Zhu, L., et al. (2016). Why do models overestimate surface ozone in the Southeast United States? *Atmospheric Chemistry and Physics*, *16*(21), 13561–13577. <https://doi.org/10.5194/acp-16-13561-2016>
- Trenberth, K. E., & Dai, A. (2007). Effects of Mount Pinatubo volcanic eruption on the hydrological cycle as an analog of geoengineering. *Geophysical Research Letters*, *34*(15), L15702. <https://doi.org/10.1029/2007GL030524>
- Van Dingenen, R., Dentener, F. J., Raes, F., Krol, M. C., Emberson, L., & Cofala, J. (2009). The global impact of ozone on agricultural crop yields under current and future air quality legislation. *Atmospheric Environment*, *43*(3), 604–618. <https://doi.org/10.1016/j.atmosenv.2008.10.033>
- Visioni, D., Pitari, G., Aquila, V., Tilmes, S., Cionni, I., Di Genova, G., & Mancini, E. (2017). Sulfate geoengineering impact on methane transport and lifetime: Results from the Geoengineering Model Intercomparison Project (GeoMIP). *Atmospheric Chemistry and Physics*, *17*(18), 11209–11226. <https://doi.org/10.5194/acp-17-11209-2017>
- Visioni, D., Slessarev, E., MacMartin, D. G., Mahowald, N. M., Goodale, C. L., & Xia, L. (2020). What goes up must come down: Impacts of deposition in a sulfate geoengineering scenario. *Environmental Research Letters*, *15*(9), 094063. <https://doi.org/10.1088/1748-9326/ab94eb>
- Vodonos, A., Awad, Y. A., & Schwartz, J. (2018). The concentration-response between long-term PM_{2.5} exposure and mortality: A meta-regression approach. *Environmental Research*, *166*, 677–689. <https://doi.org/10.1016/j.envres.2018.06.021>
- Vohra, K., Vodonos, A., Schwartz, J., Marais, E. A., Sulprizio, M. P., & Mickley, L. J. (2021). Global mortality from outdoor fine particle pollution generated by fossil fuel combustion: Results from GEOS-Chem. *Environmental Research*, *195*, 110754. <https://doi.org/10.1016/j.envres.2021.110754>
- Weisenstein, D. K., Keith, D. W., & Dykema, J. A. (2015). Solar geoengineering using solid aerosol in the stratosphere. *Atmospheric Chemistry and Physics*, *15*(20), 11835–11859. <https://doi.org/10.5194/acp-15-11835-2015>
- Weisenstein, D. K., Visioni, D., Franke, H., Niemeier, U., Vattioni, S., Chiodo, G., et al. (2022). An interactive stratospheric aerosol model intercomparison of solar geoengineering by stratospheric injection of SO₂ or accumulation-mode sulfuric acid aerosols. *Atmospheric Chemistry and Physics*, *22*(5), 2955–2973. <https://doi.org/10.5194/acp-22-2955-2022>
- World Meteorological Organization (WMO). (2022). *Scientific assessment of ozone depletion: 2022, GAW Report No. 278* (p. 509). WMO.
- Xia, L., Nowack, P. J., Tilmes, S., & Robock, A. (2017). Impacts of stratospheric sulfate geoengineering on tropospheric ozone. *Atmospheric Chemistry and Physics*, *17*(19), 11913–11928. <https://doi.org/10.5194/acp-17-11913-2017>
- Xia, L., Robock, A., Tilmes, S., & Neely, R. R., III. (2016). Stratospheric sulfate geoengineering could enhance the terrestrial photosynthesis rate. *Atmospheric Chemistry and Physics*, *16*(3), 1479–1489. <https://doi.org/10.5194/acp-16-1479-2016>
- Xu, Y., Lin, L., Tilmes, S., Dagon, K., Xia, L., Diao, C., et al. (2020). Climate engineering to mitigate the projected 21st-century terrestrial drying of the Americas: A direct comparison of carbon capture and sulfur injection. *Earth System Dynamics*, *11*(3), 673–695. <https://doi.org/10.5194/esd-11-673-2020>
- Yang, C.-E., Hoffman, F. M., Rieciuto, D. M., Tilmes, S., Xia, L., MacMartin, D. G., et al. (2020). Assessing terrestrial biogeochemical feedbacks in a strategically geoengineered climate. *Environmental Research Letters*, *15*(10), 104043. <https://doi.org/10.1088/1748-9326/abac7>
- Zeng, G., Morgenstern, O., Braesicke, P., & Pyle, J. A. (2010). Impact of stratospheric ozone recovery on tropospheric ozone and its budget. *Geophysical Research Letters*, *37*(9), L09805. <https://doi.org/10.1029/2010GL042812>
- Zhang, H., Wu, S., Huang, Y., & Wang, Y. (2014). Effects of stratospheric ozone recovery on photochemistry and ozone air quality in the troposphere. *Atmospheric Chemistry and Physics*, *14*(8), 4079–4086. <https://doi.org/10.5194/acp-14-4079-2014>